

Supporting Information

Infrared Light Dual-Excitation of Ni-Phytate-Sensitized ZnIn₂S₄ with Sulfur Vacancies for Enhanced NIR-Driven Photocatalysis

Hong Yang,^a Yuanyong Huang,^a Bifu Luo,^a Zhongkai Xie,^a Di Li,^a Dongbo Xu,^a Yong Lei,^b
Weidong Shi*^a

^a *School of Chemistry and Chemical Engineering, Jiangsu University, Zhenjiang, 212013, PR China.*

^b *Institut für Physik & IMN MacroNano (ZIK), Technische Universität Ilmenau, Ilmenau 98693, Germany.*

*Corresponding authors: swd1978@ujs.edu.cn.

1. Experimental Details

1.1 Materials

Zn(CH₃COO)₂·2H₂O(99.8%),InCl₃(99.8%),thioacetamide(TAA,99.8%),triethanolamine (TEOA, 98%), 70 wt % Phytic-acid solution, nickel acetate (Ni(Ac)₂· 4H₂O), sodium sulphate (Na₂SO₄) were obtained from Shanghai Macklin Biochemical Co. Ltd. China, absolute ethanol was obtained from Sinopharm Chemical Reagent Co., Ltd. Nafion solution (5 wt %) was purchased from Aladdin, Fluorine-doped tin oxide (FTO) coated glasses as substrates were purchased from Zhuhai Kaivo Electronic Components Co., Ltd. China. All the materials were used without further purification. Deionized water was used throughout the experiments.

1.2 Synthesis of ZIS_{1-x} monolayer

0.4 mmol Zn (CH₃COO)₂·2H₂O,0.8 mmol InCl₃ and 3.2 mmol TAA were dissolved 15 ml deionized water and 15 ml absolute ethanol with vigorous stirring for 30 min. Then, the mixture was transferred into a 50 ml Teflon-lined autoclave and heated at 180 °C for 24 h. After cooling down to room temperature, the obtained products, were collected by centrifugation, washed several times with deionized water and ethanol, and dried at 60 °C in air.

1.3 Synthesis of ZIS monolayer

0.4 mmol Zn (CH₃COO)₂·2H₂O,0.8 mmol InCl₃ and 1.6 mmol TAA were dissolved 15 ml deionized water and 15 ml absolute ethanol with vigorous stirring for 30 min. The subsequent experimental steps are the same as the synthesis of ZIS_{1-x}.

1.4 Synthesis of PA-Ni

9.95 g (0.04 mol) Ni (Ac)₂· 4H₂O was dissolved into a clean beaker containing 100 mL absolute ethanol, and steadily stirred under the water bath kept at 50 ° C. Next, 0.01 mol 70 wt% PA solution (1.432 g/mL) was put into the 50 mL absolute ethanol and cautiously added, dropwise, into the above aqueous solution. After 2 h, the light green-colored product was obtained, centrifuged at 7000 r/min and washed 5 times by ethanol to remove thoroughly residual species attached on the sample surface. Finally, the resultant solids were dried into a vacuum drying baker for overnight.

1.5 Synthesis of ZIS_{1-x} @ PA-Ni

100 mg of collected ZIS_{1-x} was put into 50 ml of ethanol and then X mg of Ni (Ac)₂· 4H₂O (x=30,37.5,49.5,75,150) was added to sonicate for 10 min, (weight ratio of ZIS_{1-x}:PA-Ni= 5:1; 4:1; 3:1; 2:1; 1:1). An appropriate amount of PA solution was dissolved in 1 ml of ethanol and slowly added dropwise into the above solution and held at 50 degrees for 4h. Finally, the mixture was centrifuged at 7000 r/min and dried into a vacuum oven.

2. Characterizations

2.1 Materials Characterization

X-ray diffraction (XRD) patterns were performed on the D/MAX-2500 diffractometer (Rigaku, Japan) operated at 40 kV and 200 mA with Cu K α ($\lambda = 0.154$ nm) radiation over the 2θ range from 5.0° to 80° at the scanning rate of $5^\circ/\text{min}$. The detailed microstructures were observed using transmission electron microscopy (TEM). The surface morphology and thickness profile were acquired on a Bruker Multimode 8 atomic force microscope (AFM) operated at the tapping mode. Fourier transform infrared (FT-IR) spectroscopy was implemented on a Nicolet NEXUS 470 spectrometer with KBr pellet technique (Thermo Electron Corporation) and the samples were prepared by the KBr pellet method. The ultraviolet-visible-near-infrared (UV-vis-NIR) diffuse reflectance spectroscopy was analyzed on a Shimadzu UV-2450 spectrophotometer and BaSO₄ was used as a reflectance standard in the wavelength range of 200–1000 nm. The binding energies and valence band (VB) were acquired using an ESCALAB 250 X-ray photoelectron spectrometer (XPS, Thermo Fisher Scientific). All the binding energies were calibrated to the C 1s peak of adventitious surface carbon at 284.8 eV. The electron spin resonance spectra were recorded on a Bruker A300 EPR spectrometer. The photoluminescence (PL) spectra and time-resolved photoluminescence spectroscopy (TRPL) under the excitation of a hydrogen flash lamp (nF900, Edinburgh Instruments) were obtained using a FLSP920 fluorescence lifetime spectrophotometer. Electrochemical measurements were performed on a CHI660E electrochemistry workstation at room temperature. Ultraviolet Photoelectron Spectroscopy (UPS, Thermo ESCALAB 250XI) was used to determine the work function of samples with -5 eV bias. All the measurements were carried out in Na₂SO₄ (0.5 M, PH = 6.8) solution and Pt wire and Ag/AgCl electrode (saturated KCl) acting as the counter and reference electrode, respectively, the fluoride tin oxide (FTO) with an active area of 1.0×2.0 cm² as the working electrode. The working electrode was prepared as follows: 10 mg of as-prepared catalysts were added into 50 μL Nafion and 2 mL ethanol mixed solution, which was then uniformly spin-dropped onto a clean 1 cm \times 2 cm fluorine-doped tin oxide (FTO) glass electrode using a spin coater (MODEL KW-4A, Shanghai, China). Subsequently, the FTO-coated glass was dried at room temperature.

2.2 Photocatalytic hydrogen (H₂) evolution activity

The photocatalytic H₂ evolution activity was carried out in a 250 ml Pyrex top-irradiation photo-reactor connected to a closed gas-circulation system using a 300 W Xe lamp equipped with an 800 nm cut-off filter at 20 °C. 20 mg photo-catalyst was dispersed in 50 ml aqueous solution containing 10 ml TEOA as sacrificial reagents in a Pyrex flask. After a 30 min degassing pretreatment, the suspension was irradiated for 5 h and the amount of H₂ was analyzed using an on-line gas chromatograph (the system was purged with Ar equipped with a Shimadzu GC-14C gas chromatograph). To evaluate the H₂ evolution stability, the system was evacuated every five hours and the released H₂ amount was recorded at intervals of 1 h by totally recycling test for 20 h.

3. Supplementary Figures and Tables

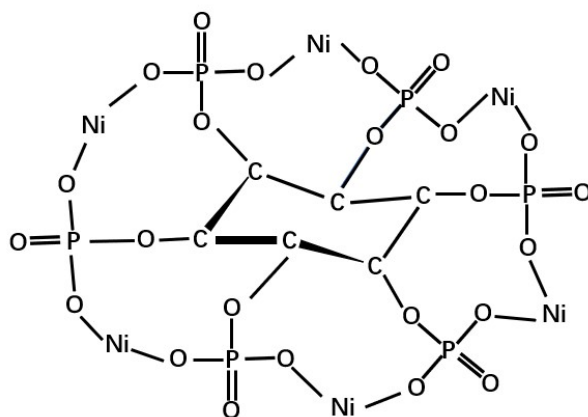


Figure S1. Plausible PA-Ni complex structure.

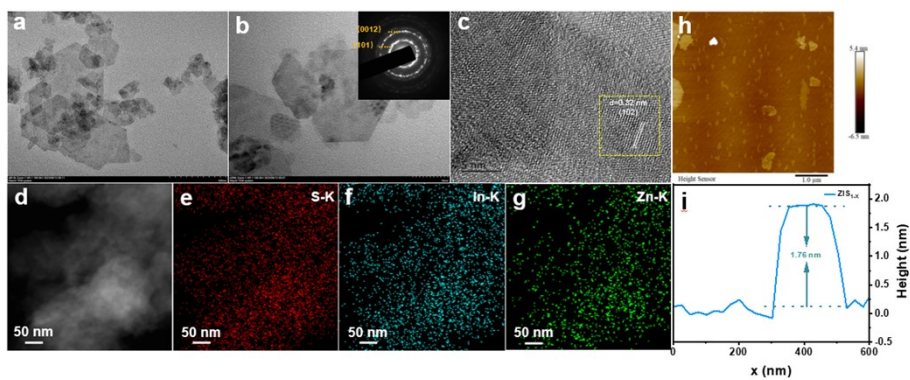


Figure S2. (a) and (b) TEM image of ZIS_{1-x} , (c) HRTEM image, (d) high angle annular dark-field (HAADF) scanning TEM image, (e), (f) and (g) the elemental mapping images, (h) AFM image, and (i) the corresponding height profiles of ZIS_{1-x} .

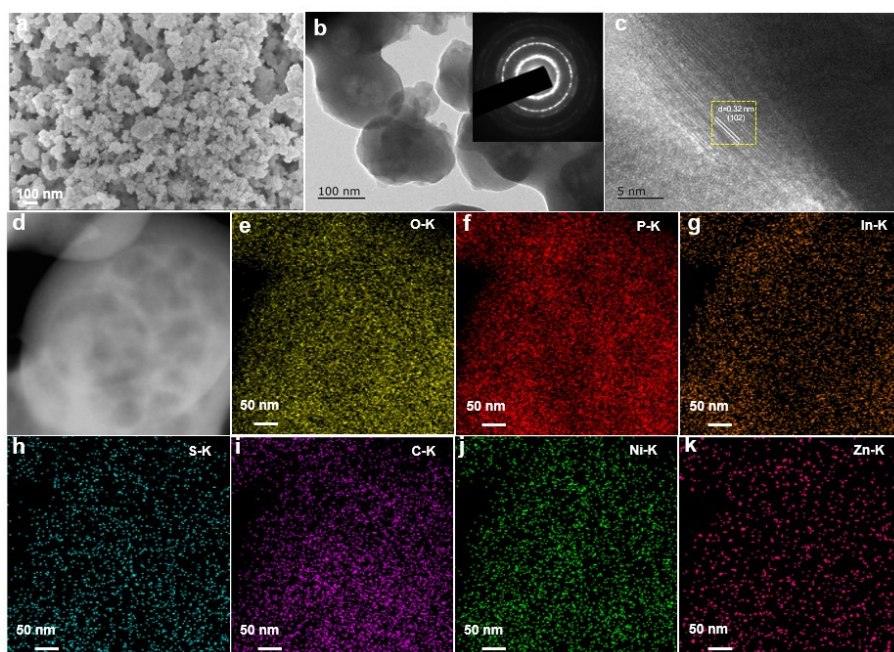


Figure S3. (a) SEM image of PA-Ni, (b) TEM image of ZIS_{1-x}@PA-Ni_(2:1), (c) HRTEM image, (d) high angle annular dark-field (HAADF) scanning TEM image, (e-k) the elemental mapping images.

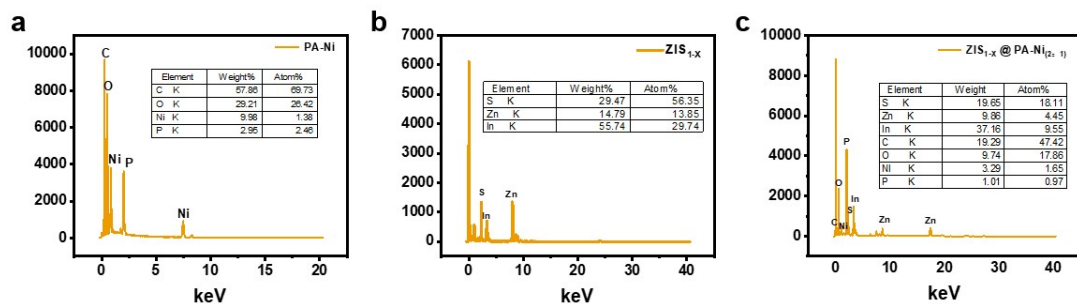


Figure S4. The EDS analysis of PA-Ni, ZIS_{1-x} and ZIS_{1-x}@PA-Ni_(2:1).

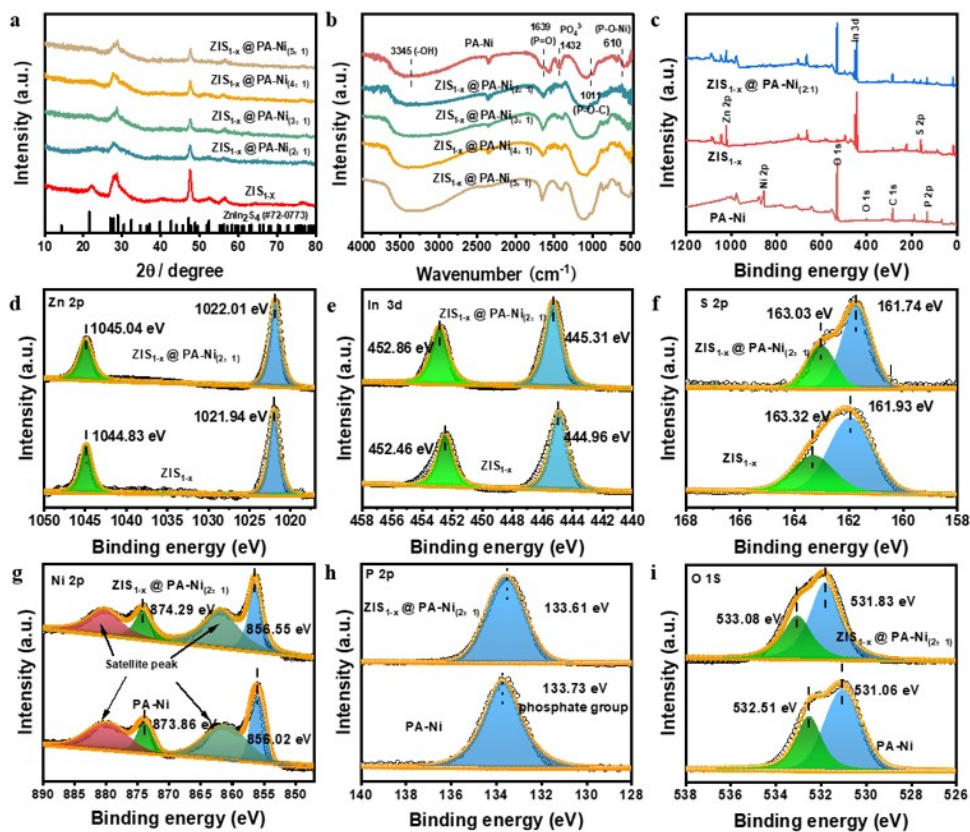


Figure S5. (a) XRD spectra; (b) FT-IR spectra; (c) XPS spectra; (d) Zn 2p XPS spectra; (e) In 3d XPS spectra; (f) S 2p XPS spectra; (g) Ni 2p XPS spectra; (h) P 2p XPS spectra; (i) O 1s XPS spectra.

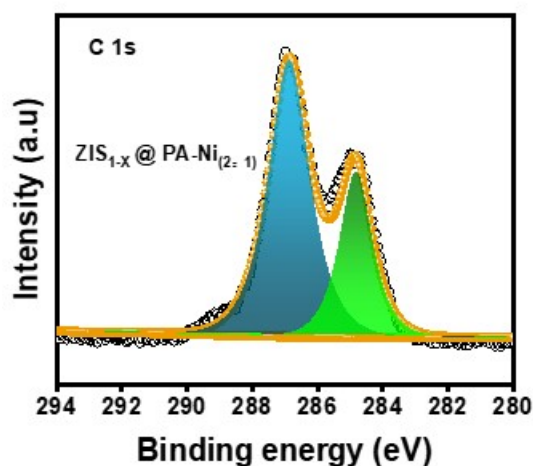


Figure S6. C 1s 2p XPS spectra.

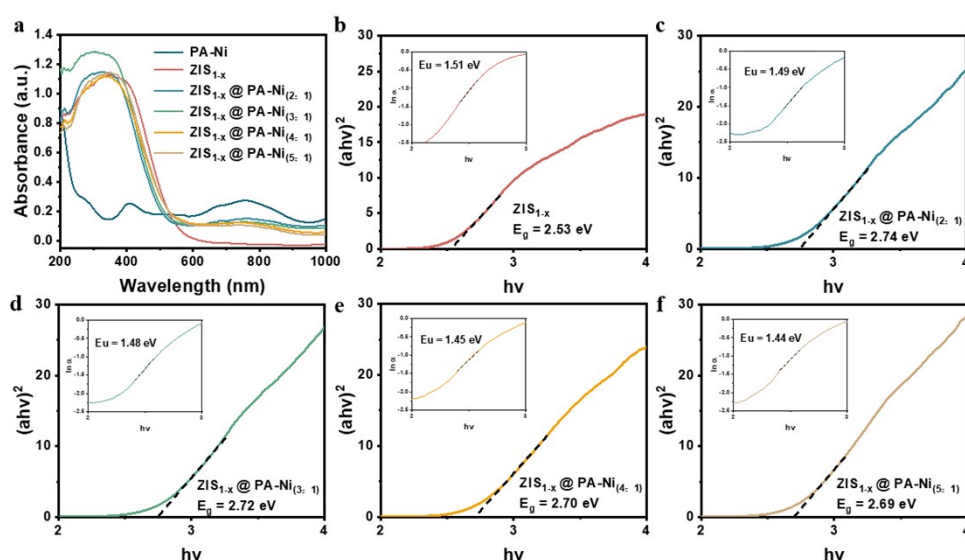


Figure S7. (a) UV-visible spectra; (b-f) Bandgap energy (E_g) calculated from the absorption spectra. The inset is The Urbach plots, from which the Urbach energy (E_u) can be obtained. By plotting the absorption edge data using Urbach, an approximate estimation of the band tails of the mid-gap states can be made, which is expressed as:

$$\alpha = \alpha_0 \exp(h\nu/E_u)$$

where α is absorption coefficient, α_0 is a constant, $h\nu$ is the incident photon energy, and E_u denotes the energy of the band tail or sometimes called the Urbach energy. The E_u values were calculated from the inverse of the slope of $\ln \alpha$ versus $h\nu$.^{1,2}

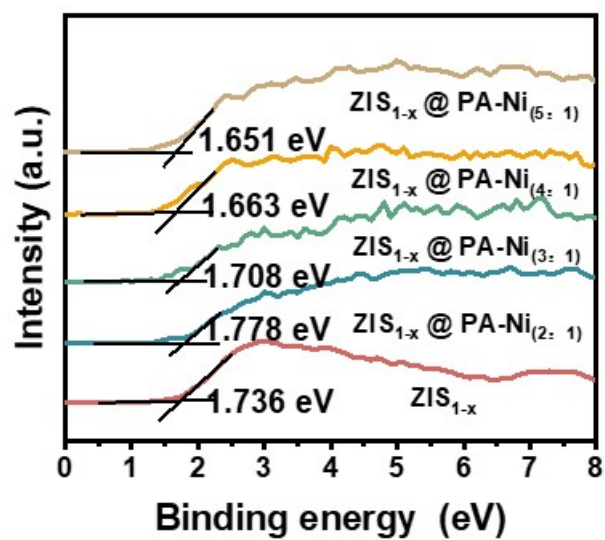


Figure S8. XPS valence band spectra.

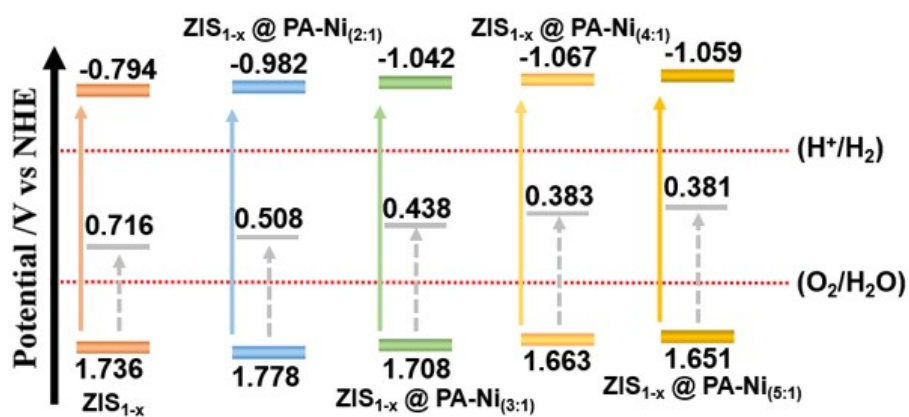


Figure S9. The schematic diagram of the energy band structure.

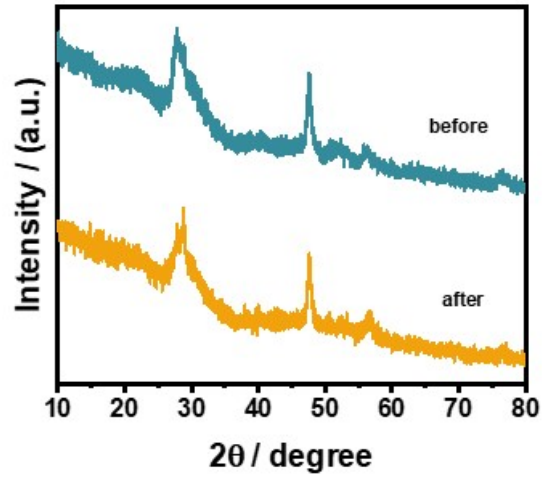


Figure S10. XRD spectra of ZIS_{1-x} @ PA-Ni_(2:1) sample before and after the photocatalytic reaction under the $\lambda > 800$ nm.

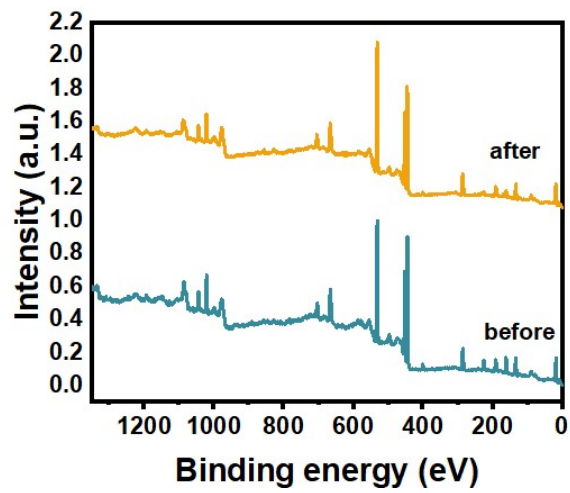


Figure S11. XPS spectra of ZIS_{1-x} @ PA-Ni_(2:1) sample before and after the photocatalytic reaction under the $\lambda > 800$ nm.

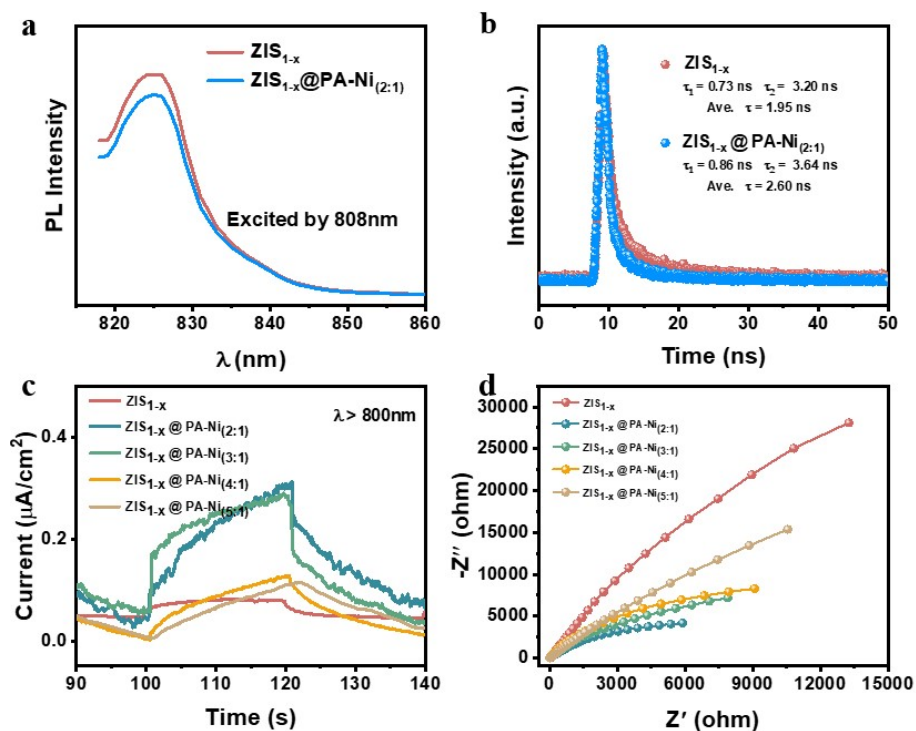


Figure S12. (a) PL spectra; (b) TRPL decay spectra; (c) Periodic on/off photocurrent responses at $\lambda > 800$ nm; (d) EIS spectra.

The average PL lifetime (τ_A) could be calculated according to the equation:³

$$\tau_A = \frac{A_1\tau_1^2 + A_2\tau_2^2}{A_1\tau_1 + A_2\tau_2}$$

where τ_1 and τ_2 are the fluorescence lifetimes and A_1 and A_2 are the corresponding amplitudes.

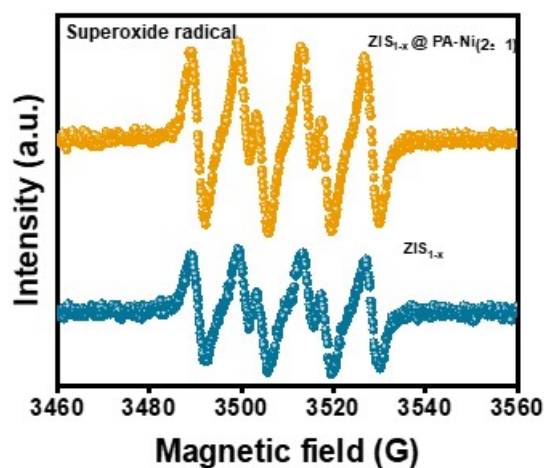


Figure S13. DMPO spin-trapping EPR spectra under the visible NIR.

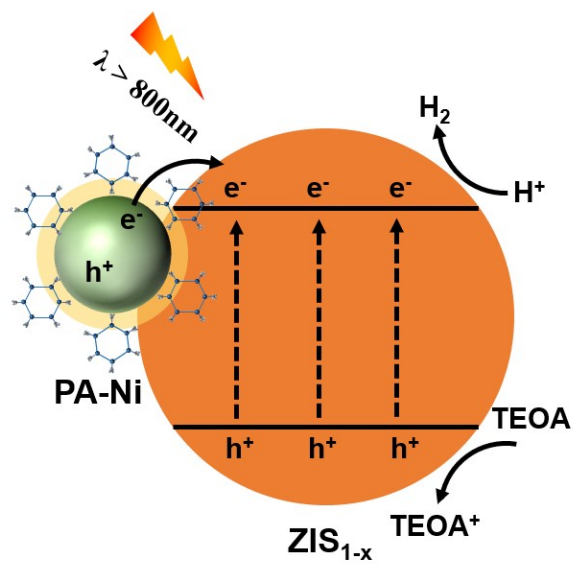


Figure S14. Possible mechanism of photocatalytic H₂ evolution over ZIS_{1-x} @ PA-Ni (2:1) composite under NIR illumination.

Table S1. Summary and comparison of different photocatalytic systems under NIR light irradiation the photocatalytic H₂ evolution activity.

Catalytic System	Cocatalyst	Optical Absorption (nm)	NIR Photoactivity	Ref.
PA-Ni @ ZIS _{1-x}	-	$\lambda > 800$	119.85 $\mu\text{mol/g/h}$	This work
CNS / g-C ₃ N ₄	-	$\lambda > 800$	0.32 $\mu\text{mol/g/h}$	4
g-C ₃ N ₄ / UFR-NC _{0.02}	3 wt% Pt	$\lambda > 800$	9 $\mu\text{mol/g/h}$	5
HOCN	1 wt% Pt	$\lambda > 800$	91 $\mu\text{mol/g/h}$	6
Pt @ CdS NPs / Zn-TCPP NSs	2 wt% Pt	$\lambda > 800$	20 $\mu\text{mol/g/h}$	7
NYF @ ZIS	1wt% Pt	$\lambda > 800$	17.8 $\mu\text{mol/g/h}$	8
PA-Ni @ PCN	-	$\lambda > 800$	27 $\mu\text{mol/g/h}$	9
Ag ₂ S / CdS / Cd ₂ SO ₄ (OH) ₂	-	$\lambda > 800$	0.3 $\mu\text{mol/g/h}$	10
S-doped g-C ₃ N ₄	-	$\lambda > 800$	17.46 $\mu\text{mol/g/h}$	11

1 F. Urbach, *Phys. Rev.*, 1953, **92**, 1324–1324.

2 H. Mahr, *Phys. Rev.*, 1963, **132**, 1880–1884.

3 Z. Zhang, J. Huang, Y. Fang, M. Zhang, K. Liu and B. Dong, *Advanced Materials*, 2017, **29**, 1606688.

4 W. Wang, Y. Tao, L. Du, Z. Wei, Z. Yan, W. K. Chan, Z. Lian, R. Zhu, D. L. Phillips and G. Li, *Applied Catalysis B: Environmental*, 2021, **282**, 119568.

5 H. Che, G. Che, P. Zhou, C. Liu, H. Dong, C. Li, N. Song and C. Li, *Chemical Engineering Journal*, 2020, **382**, 122870.

6 S. Li, C. Hu, Y. Peng and Z. Chen, *RSC Adv.*, 2019, **9**, 32674–32682.

7 Z. Xia, R. Yu, H. Yang, B. Luo, Y. Huang, D. Li, J. Shi and D. Xu, *International Journal of Hydrogen Energy*, 2022, **47**, 13340–13350.

8 Z. Chen, Y. Shi, J. Lu, L. Cao, Y. Tian, L. Chen, F. Guo and W. Shi, *Journal of Environmental Chemical Engineering*, 2022, **10**, 108352.

9 Y. Huang, Y. Jian, L. Li, D. Li, Z. Fang, W. Dong, Y. Lu, B. Luo, R. Chen, Y. Yang, M. Chen and W. Shi, *Angewandte Chemie International Edition*, 2021, **60**, 5245–5249.

10 X. Zhang, T. Liu, F. Zhao, N. Zhang and Y. Wang, *Applied Catalysis B: Environmental*, 2021, **298**, 120620.

11 X. Wu, D. Li, B. Luo, B. Chen, Y. Huang, T. Yu, N. Shen, L. Li and W. Shi, *Applied Catalysis B: Environmental*, 2023, **325**, 122292.